Received: 24 May 2017 | Accepted: 24 May 2017
DOI: 10.1002/jcp.26031

ORIGINAL RESEARCH ARTICLE

WILEY Journal of Cellular Physiology

The nucleus is irreversibly shaped by motion of cell boundaries in cancer and non-cancer cells

Vincent J. Tocco[1] | Yuan Li[1] | Keith G. Christopher[1] | James H. Matthews[2] | Varun Aggarwal[1] | Lauren Paschall[1] | Hendrik Luesch[2] | Jonathan D. Licht[3] | Richard B. Dickinson[1] | Tanmay P. Lele[1,4]

[1] Department of Chemical Engineering, University of Florida, Gainesville, Florida

[2] Department of Medicinal Chemistry, Center for Natural Products, Drug Discovery and Development (CNPD3), University of Florida, Gainesville, Florida

[3] Division of Hematology and Oncology, Department of Medicine, University of Florida Health Cancer Center, Gainesville, Florida

[4] Department of Anatomy and Cell Biology, University of Florida College of Medicine, Gainesville, Florida

Correspondence
Tanmay P. Lele, Department of Chemical Engineering, Bldg. 723, University of Florida, Gainesville, FL 32611.
Email: tlele@che.ufl.edu

Funding information
National Science Foundation, Grant number: CMMI 1437395; National Institutes of Health, Grant numbers: R01 EB014869, R01 GM102486, U54CA193419, R01 CA172310

Actomyosin stress fibers impinge on the nucleus and can exert compressive forces on it. These compressive forces have been proposed to elongate nuclei in fibroblasts, and lead to abnormally shaped nuclei in cancer cells. In these models, the elongated or flattened nuclear shape is proposed to store elastic energy. However, we found that deformed shapes of nuclei are unchanged even after removal of the cell with micro-dissection, both for smooth, elongated nuclei in fibroblasts and abnormally shaped nuclei in breast cancer cells. The lack of shape relaxation implies that the nuclear shape in spread cells does not store any elastic energy, and the cellular stresses that deform the nucleus are dissipative, not static. During cell spreading, the deviation of the nucleus from a convex shape increased in MDA-MB-231 cancer cells, but decreased in MCF-10A cells. Tracking changes of nuclear and cellular shape on micropatterned substrata revealed that fibroblast nuclei deform only during deformations in cell shape and only in the direction of nearby moving cell boundaries. We propose that motion of cell boundaries exert a stress on the nucleus, which allows the nucleus to mimic cell shape. The lack of elastic energy in the nuclear shape suggests that nuclear shape changes in cells occur at constant surface area and volume.

KEYWORDS
cell forces, nuclear mechanics, nuclear shape

1 | INTRODUCTION

The nucleus undergoes changes in its shape as a cell migrates through tissue and tight spaces (Denais et al., 2016; McGregor, Hsia, & Lammerding, 2016), but how the nuclear deformation is caused by changes in cell shape is not well understood. Yet, the mechanism of nuclear deformation is important, given that the extent of nuclear deformation limits cell migration through extracellular matrix (Petrie, Koo, & Yamada, 2014), may change chromatin architecture, and consequently gene expression (Gupta, Marcel, Sarin, & Shivashankar, 2012; Thomas, Collier, Sfeir, & Healy, 2002; Vergani, Grattarola, & Nicolini, 2004).

Furthermore, in many forms of cancer, the nucleus commonly has shape abnormalities, including lobes, invaginations and folds (Chow, Factor, & Ullman, 2012). Abnormalities in nuclear shape occur early in tumor progression (Boyd, Pienta, Getzenberg, Coffey, & Barrett, 1991) and help improve the accuracy of prognosis in clinical settings (Bloom & Richardson, 1957). Nuclear shape abnormalities correlate with the biological behavior and clinical prognosis of different cancers

Vincent J. Tocco and Yuan Li contributed equally to this work.

(Bussolati, Marchiò, Gaetano, Lupo, & Sapino, 2008; Elston & Ellis, 1991). Despite the strong diagnostic and prognostic importance of nuclear shape abnormalities (Giardina et al., 1996; Haroske et al., 1996), the mechanism by which the nucleus becomes abnormally deformed in cancer is not understood.

Nuclear deformation is a response of the nucleus to mechanical stresses. In some models explaining the correlation between nuclear shape and cell shape, impinging actomyosin impinging actomyosin stress fibers exert compressive stress on the nucleus. The stress exerted by these fibers causes an elastic deformation of the nucleus such that it can become elongated starting from an approximately spherical shape (Khatau et al., 2009; Versaevel, Grevesse, & Gabriele, 2012). In this model, nuclear shape is determined by the distribution and magnitude of the forces generated by the stress fibers and the elastic properties of the nucleus. No time history of the stresses is required to explain the current nuclear shape; instantaneous cell shape determines the instantaneous nuclear shape.

Here, we show that both fibroblast nuclei and cancer nuclei in spread cells do not store elastic energy, challenging the current models of nuclear shaping. Further, we show that a change in cell shape is required for deformation of the nucleus during cell migration. Based on these results, we propose that motion of the cell boundary transmits a stress to the nuclear surface to shape the normal nucleus and to amplify shape abnormalities in the cancer nucleus.

2 | MATERIALS AND METHODS

2.1 | Cell culture and transfection

All cells were maintained in a humidified incubator at 37°C and 7% CO_2. Mouse fibroblasts (MEF and NIH 3T3) were cultured in Dulbecco's modified Eagle's medium (DMEM) with 4.5 g/L of glucose (Mediatech, Manassas, VA), supplemented with 10% donor bovine serum (DBS; Gibco, Grand Island, NY) and 1% penicillin/streptomycin (Mediatech). Human breast cancer cells (MDA-MB-231) were cultured in 4.5 g/L glucose DMEM without HEPES and L-glutamine (Invitrogen, Carlsbad, CA), supplemented with 10% (v/v) donor bovine serum (DBS, Gibco), 1% (v/v) 100× MEM non-essential amino acid (Mediatech), 1% (v/v) 200 mM L-glutamine (Fisher Scientific, Hampton, NH), and 1% Penicillin-Streptomycin (Mediatech). Human breast epithelial cells (MCF-10A) were cultured in DMEM/F12 (Invitrogen), supplemented with 5% (v/v) horse serum (Invitrogen), 1% Penicillin-Streptomycin (Mediatech), 20 ng/ml epidermal growth factor (EGF, Peprotech, Rocky Hill, NJ), 0.5 μg/ml hydrocortisone (Sigma–Aldrich, St. Louis, MO), 100 ng/ml cholera toxin (Sigma–Aldrich), and 10 μg/ml insulin (Sigma–Aldrich). Cells were seeded onto 35 mm glass-bottom dishes (WPI, Sarasota, FL) treated with 5 μg/ml fibronectin (BD Biosciences, San Jose, CA) or hydrophilic polymer tissue culture dishes (described below; Ibidi, Martinsreid, Germany). For 3D culture, cells were encapsulated in 3 mg/ml rat-tail collagen I gels (Ibidi), as specified by the manufacturer. Briefly, 5 mg/ml solution of collagen was thawed, diluted, and brought to physiological pH with 1 M sodium hydroxide. The cells were suspended in this solution and transferred to a culture dish. Collagen fibers were allowed to polymerize at 37°C for 30 min before cell culture. Transfections of were performed with Lipofectamine 3000 (ThermoFisher Scientific, Waltham, MA) in OptiMEM serum-free media (ThermoFisher) following the manufacturer's protocols. Dendra2-H3.3-N-14 construct was a gift from Michael Davidson (Addgene, plasmid #57725). RFP-Lifeact was obtained from Ibidi (#60102). EGFP-Tubulin was a gift from Patricia Wadsworth (Addgene, plasmid #12298). GFP-NLS was a gift from Alexander Ishov and GFP-KDEL and GFP-SUN1L-KDEL were gifts from Kyle Roux.

2.2 | Nuclear excision

The nucleus was removed from NIH 3T3 or MDA-MB-231 cells by using a 0.5 μm micropipette tip (Femtotip; Eppendorf North America, Hauppauge, NY) as a scalpel. The micropipette tip was controlled with an Eppendorf InjectMan micromanipulator system. SYTO11 dye (ThermoFisher) was used at manufacturer-recommended concentrations to label the nuclei of MDA-MB-231 cells.

2.3 | Microcontact printing

Hydrophilic polymer tissue culture dishes (Ibidi, Martinsreid, Germany) were patterned by microcontact printing as previously described (Csucs, Michel, Lussi, Textor, & Danuser, 2003; Théry & Piel, 2009). Briefly, specified features were etched on a silicon wafer surface using standard photolithography techniques. Then, Sylgard 184 (Polydimethylsiloxane Elastomer Kit; Dow Corning, Midland, MI) was mixed in a 10:1 base-to-crosslinking agent ratio and cured at 60°C for 1 hr on the silicon wafer. The cured elastomer was peeled from the silicon wafer and cut into stamps. Rhodamine-conjugated fibronectin (Cytoskeleton, Denver, CO) was diluted to 50 μg/ml in deionized water and a 20 μl drop was applied to adsorb on the stamp surface for 1 hr. Culture dishes were treated briefly with a hand-held corona treater (Model BD-20; Electro-Technic Products, Inc., Chicago, IL) to increase fibronectin transfer before printing the surface with rinsed and dried stamps. Non-printed regions of the dish were backfilled with 0.2 μg/ml poly-L-lysine grafted with poly-ethylene glycol (PLL-g-PEG Surface Solutions, Dübendorf, Switzerland) in phosphate buffered saline (PBS) for 1 hr to prevent unwanted protein adsorption. Substrates were stored for up to 1 week at 4°C in PBS.

2.4 | Cell staining, and fixed and live cell imaging

For fixed-cell experiments, cells were fixed in 4% paraformaldehyde at room temperature (25°C) for 10 min, washed with PBS, and stained with Hoechst 33342 and fluorescent phalloidin to label DNA and F-actin, respectively. Imaging was done using a Nikon A1 laser scanning confocal microscope (Nikon, Melville, NY) with a 60×/1.4NA oil immersion objective. For live cell imaging, cells were maintained at 37°C and 5% CO_2 in a humidified chamber. Z-stacks were acquired with a 0.3-μm axial step size for fixed cell imaging, and 1–2-μm axial step size for live cell imaging.

2.5 | High-content imaging

Both MDA-MB-231 and MCF-10A cells were seeded on 384-well plates and then fixed at approximately 95% confluence. The nuclei were stained with Hoechst 33342 dye and imaged with an Operetta CLS system (PerkinElmer, Waltham, MA) with a consistent intensity of UV light. The images were analyzed by Cell Profiler software (Carpenter Lab, Boston, MA) to acquire data of nuclear morphology and signal intensity.

2.6 | Image analysis and nuclear measurements

Fiji software (Schindelin et al., 2012) was used for image processing and nuclear measurements. For 2D nuclear measurements, either the nuclear outline was traced manually (for experiments without fluorescence) or the nuclear parameters determined automatically from applying an intensity threshold to maximum intensity XY nuclear projections of fluorescent nuclei. Nuclear contour ratio of cancer cells was calculated as $4\pi A/P^2$, where A is the area and P is the perimeter of the maximum intensity projection. To measure nuclear 3D irregularity, nuclear volume was measured in FIJI with the "3D objects counter" with applied intensity threshold and the x-y coordinate of all pixels counted for measurement of nuclear volume were exported by FIJI. With these coordinates, a convex hull was fit to the nucleus using Anaconda Python with integrated code. 3D irregularity is the difference in the convex hull volume and the nuclear volume, normalized by the nuclear volume.

3 | RESULTS

3.1 | Deformed nuclear shapes do not store elastic energy

Nuclear shapes commonly conform to cell shapes. For example, nuclei are elongated in cells with extended morphologies (e.g., elongated fibroblasts or endothelial cells), and more circular in symmetrical cells (e.g., in the renal epithelium of proximal tubules (Gundersen & Worman, 2013; Webster, Witkin, & Cohen-Fix, 2009). What causes conformity of nuclear shape to cell shape? If nuclear shape is completely determined by cell shape, irrespective of the history of cell shape deformations, then removal of cellular stresses should cause an elastic relaxation of nuclear shape to the unstressed (approximately spherical) shape. Another possibility is that the nuclear shape is the cumulative result of *irreversible* nuclear deformations caused by cell shape deformations over time (Li et al., 2015).

To distinguish between these possibilities, we physically separated elongated nuclei in mouse embryonic fibroblasts (MEF) from the surrounding cytoplasm to remove any cellular stresses, and looked for elastic relaxation of nuclear shape. Nuclei were microdissected from cell bodies with a fine micropipette, such that surrounding cell components were cut away from the nucleus (Figure 1a). This method enabled us to measure the shape of the same nucleus before and after isolation from the cell, which is not possible in other methods that involve chemical digestion and centrifugation (Deguchi, Maeda, Ohashi, & Sato, 2005). Cytoskeletal elements were confirmed to be completely absent from the area around the dissected nucleus (Supplementary Figure S1). We tracked the nuclear shape for up to 10 min following isolation, which is much longer than the few seconds expected for elastic nuclear relaxation (Neelam et al., 2015). Yet, the nuclear shape (quantified by cross-sectional area and elongation) was unchanged after separation from the cell body (Figure 1a). This suggests that nuclear elongation is an irreversible deformation and cellular forces that deformed the nucleus have dissipated and are not static.

We further tested whether nuclear shapes store elastic energy in cancer cells, in which nuclear shapes are typically highly abnormal (Zink, Fischer, & Nickerson, 2004). We micro-dissected the cell body of MDA-MB-231 (human breast cancer epithelial) cells and found that abnormalities of the nuclear contour were unchanged after the

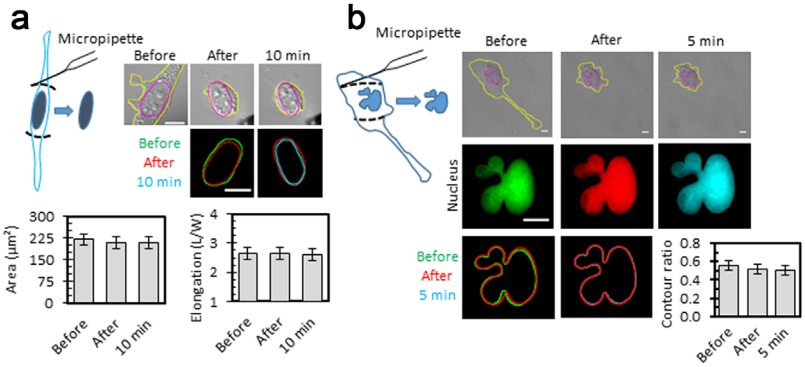

FIGURE 1 Nuclear shape is not a result of elastic deformation caused by static cytoskeletal stresses. (a) Shown is a schematic representation of the excision of the MEF nucleus from the cell body, and typical experimental images, with the nuclear outlines marked in magenta and cell outlines marked in yellow. "Before" and "After" refer to immediately before and immediately after the nuclear excision, respectively. The excised nucleus is also shown 10 min following the excision. Overlays show nuclear outlines (scale bars: 10 μm). Nuclear area and elongation (quantified as length, L, over width, W) before, after, and 10 min after excision with the micropipette are shown; data are means ± SEM for measurements of 16 separately excised nuclei. (b) Shown is a typical microdissection experiment with an MDA-MB-231 (human breast cancer) cell along with contour ratio of the nucleus before, after, and 5 min after excision. Data are means ± SEM for measurements of 10 separately excised nuclei. Color coding is as in panel a

surrounding cell body was cut away (Figure 1b). We compared the nuclear contour ratio (a measure of abnormality; see methods) before and after nuclear isolation, and found no statistically significant effect of the isolation on the contour ratio (Figure 1b). The lack of elastic relaxation upon removal of the surrounding cell implies that the deformed nuclear shape in these different cell types stores no elastic energy and that the deformation is not an elastic response to the instantaneous cell shape-dependent cytoskeletal forces on the nucleus.

3.2 | The deforming cell boundary elongates the fibroblast nucleus

How is conformity between cell and nuclear shapes established? Since nuclear deformations in spread cells are irreversible, we hypothesized that the *changes* in cellular shape may exert dissipative forces that irreversibly deform the nucleus. To test this hypothesis, we designed micropatterns consisting of thin (5-μm wide) lines of varying lengths, and used microcontact printing to create fibronectin-patterned substrates. We simultaneously tracked dynamic deformations of nuclear and cellular shapes in fibroblasts as they spread along these lines. As anticipated, nuclei were more elongated in longer cells than in shorter cells at steady state (Supplementary Figure S2). Early in the spreading process, nuclear elongation proceeded with cell spreading (Figure 2a). During this early phase of cell spreading, actomyosin bundles are undeveloped (Li et al., 2015), thus are likely not responsible for nuclear elongation. On micropatterned lines that were sufficiently long, nuclear elongation slowed and ultimately stopped while the cell continued to spread (Figure 2b,c), suggesting an asymptotic mechanical limit to nuclear elongation. However, on shorter lines where cell spreading was constrained to a fixed length (Figure 2b, c), nuclear elongation stopped abruptly upon the cessation of cell spreading, with a resulting steady-state nuclear length shorter than the above asymptotic limit. These observations show that cell spreading must proceed in order for nuclear deformation to continue.

During cell spreading on thin lines in the above experiments, movements of nuclear boundaries occurred in the same direction as the movements of the corresponding cell boundaries located in the direction normal to the nuclear boundary (Figure 2a). That is, nuclei elongated in the direction of cell spreading and were compressed laterally (not quantified) as the cell narrowed in the direction perpendicular to the fibronectin line. To test this idea

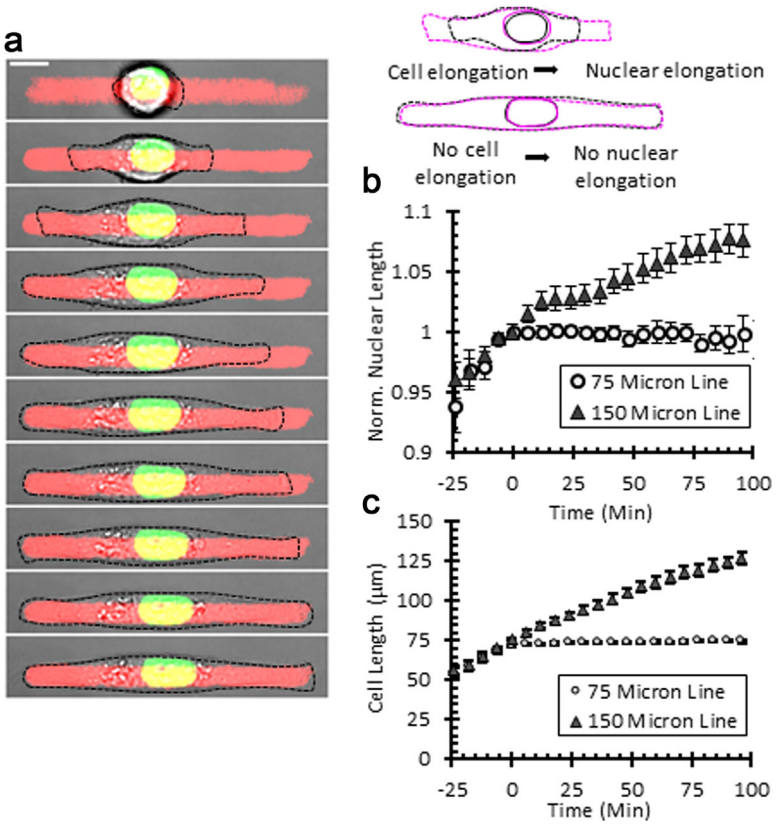

FIGURE 2 The dynamics of nuclear shaping during cell spreading. (a) Images show dynamic spreading of an NIH3T3 cell expressing Dendra2-histone H3.3 on a 75-μm long fibronectin line (scale bar: 10 μm). Nuclear deformation is schematically shown by overlaid outlines of the cell and the nucleus. (b and c) Nuclear and cell lengths are plotted against the time of cell spreading, respectively. The time at which the cell reached 75 μm in length was designated as $t = 0$, and the nuclear length data were normalized to nuclear length at $t = 0$ ($n = 16$ for 75 μm line, and 18 for 150 μm line). Error bars are standard error of the mean

further, we next examined the correlation between the deformations in the nuclear and cellular shapes as cells migrated between thin and wide fibronectin patterns. We tracked cells along a fibronectin micropattern (Chang, Guo, Kim, & Wang, 2013) consisting of a 400 μm line terminating in a 50 × 100 μm^2 ("2D") rectangle (Figure 3a). As the cell crawled onto the rectangular region, the nuclear shape was initially unchanged, despite widening of the cell shape at the cell front (Figure 3b, left panels; compare −28′ with −56′). Only when the cell width expanded laterally (i.e., perpendicular to the cell axis, 0′) in the region adjacent to the nuclear surface did the nucleus begin to widen (Figure 3b, left panels, and movie 1). Similarly, for cells moving from wide to thin fibronectin regions, the nucleus compressed laterally only when the adjacent cell edge moved laterally towards the nucleus (Figure 3b, right panels; compare −28′ with 0′ and 28′). To quantify these observations, we measured nuclear width and compared it with cell width at two positions (at the nuclear midline and 35 μm from the nucleus into the leading edge) as the nucleus progressed from the line to the 2D region (Figure 3c). Nuclear width did not change despite the increase in cell width at the cell front; rather, the expansion of the nuclear width precisely coincided with the increase in cell width lateral to the nucleus. Nuclear deformation occurred only when the cell deformed; moreover, global changes in cell shape did not affect the nuclear shape unless a nearby membrane was moving in a direction normal to the nuclear surface.

To examine the generality of these observations, we tracked deformations in nuclear shape of NIH 3T3 fibroblasts migrating in reconstituted collagen gels, and observed similar instances of nuclear widening in direct response to cell widening (Supplementary Figure S3). There, a narrow, elongated cell became wider as it migrated in the local extracellular matrix environment, and the deformations in the nuclear shape coincided with the deformations in cell shape perpendicular to the nuclear surface. Such observations are consistent

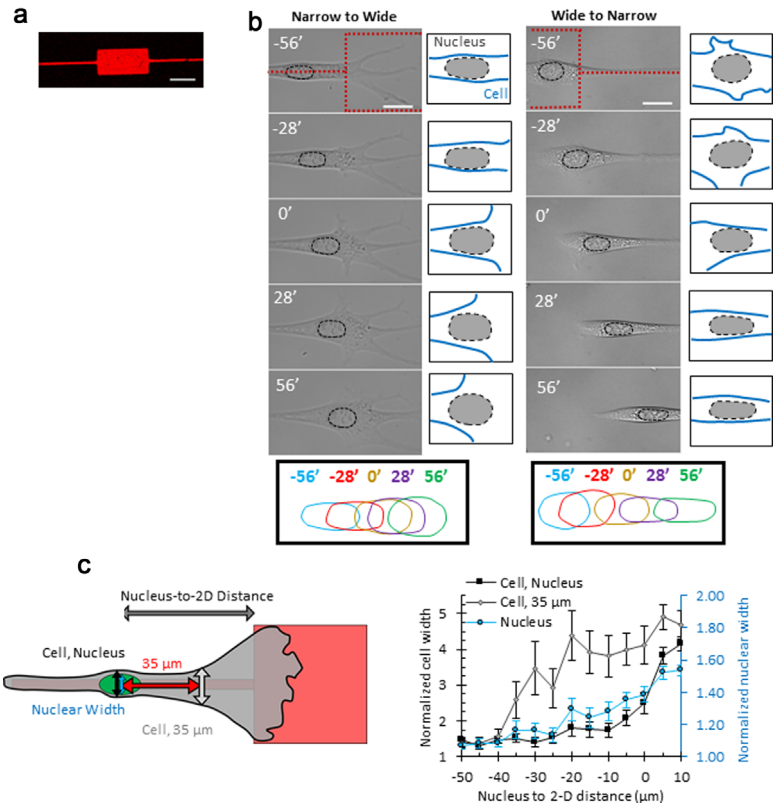

FIGURE 3 Dynamic deformation of the fibroblast nucleus during cell migration. (a) Shown is an example of a rhodamine-fibronectin micropattern consisting of a 5 μm wide line connected to a 2D rectangle measuring 100 × 50 μm^2 (scale bar: 50 μm), along with time lapse images (b) of cells migrating between micropattern regions, with narrow-to-wide (left) and wide-to-narrow (right) transitions. Nuclei (black dotted lines), cell outlines (blue), and the fibronectin pattern (red dotted lines) are outlined for clarity. The time at which the nucleus crossed the interface of the fibronectin regions was designated as $t = 0$ (scale bar: 20 μm). Below: Overlaid nuclear outlines at different time points (different color for each time). (c) Nuclear width ("nucleus"), cell width at the nuclear midline ("cell, nucleus"), and cell width 35 μm from the nuclear midline toward the leading cell edge ("cell, 35 μm") were measured as shown in the schematic diagram on the left. The data are plotted against the distance between the nuclear midline and edge of the 2D region (dark gray arrow, top). The origin of the *x*-axis corresponds to the nuclear midline reaching the edge of the 2D region. Data are means pooled from seven narrow-to-wide transitions and all width measurements are normalized to the minimum nuclear width. Error bars represent SEM for all data points, binned into increments of 5 μm of nucleus to 2D distance

with the transitions observed on micropatterned lines and again suggest that local motion of the cell boundary is required for changing nuclear shape.

3.3 | The deforming cell shape amplifies cancer nuclear abnormalities

We quantitatively measured nuclear shape abnormalities during cancer cell spreading by imaging nuclei expressing GFP-NLS in MCF-10A and MDA-MB-231 cells (Figure 4a). We measured the deviation of the nucleus from a convex shape to calculate 3D irregularity (see Figure 4b and Methods). The 3D irregularity increased in cancer nuclei during spreading of cancer cells, but decreased in MCF-10A cells (Figure 4b).

We asked if abnormal cancer shapes are heritable. We classified regular and irregular nuclei in MDA-MB-231 cells, tracked them through mitosis, and quantified the proportion of regular or irregular daughter nuclei (Supplementary Figure S4). Cells with irregular nuclei were more likely to divide into daughter cells with irregular nuclei; cells with regular nuclei were more likely to divide into daughter cells with regular nuclei (Supplementary Figure S4). These results suggest that nuclear abnormalities are heritable from mother to daughter cells. An obvious reason for this observation could be the degree of ploidy in cells. Therefore, we quantified the DNA content in MCF-10A and MDA-MB-231 nuclei using high-content imaging of Hoechst 33342 DNA. Computing histograms for total fluorescence intensity showed a bimodal distribution in MCF-10A cells, consistent with proportions expected from the cell cycle, while MDA-MB-231 cells expectedly had a higher DNA content (Supplementary Figure S5a). However, we found no dependence of nuclear irregularity on total DNA content in either MCF-10A or MDA-MB-231 cells (Supplementary S5b). Therefore, ploidy is not necessarily a factor in determining abnormal cancer nuclear shapes.

4 | DISCUSSION

The shape of the nucleus inside the cell has been commonly assumed to store elastic energy. That is, the rounded nucleus in a suspended cell becomes elongated or flattened in a spreading cell through an elastic (i.e., reversible) deformation of the nucleus. Such a model predicts that removing cytoplasmic forces on the nucleus should restore the original rounded shape of the nucleus. Similarly, nuclear lobes and invaginations characteristic of cancer nuclei might be considered to be elastically deformed in response to cytoskeletal forces (Funkhouser et al., 2013). Here we showed that micro-dissection of the nucleus from the cell does not cause a relaxation of the nuclear shape. The lack of elastic relaxation upon removal of the surrounding cell implies that the deformed nuclear shape in these different cell types stores no elastic energy and that the deformation is not an elastic response to the instantaneous cell shape-dependent cytoskeletal forces on the nucleus.

Pajerowski, Dahl, Zhong, Sammak, and Discher (2007) aspirated nuclei and cells into a micropipette and measured deformed nuclear shapes. Upon ejecting the nucleus and cell from the pipette, they found that the nuclear shape remained deformed. However, inside cells, the nucleus does not undergo rapid and large deformations like those applied in that study (100–500% strain in a few seconds). Therefore, these experiments do not necessarily explain the irreversibility of elongated nuclear shapes in cells that are established by the process of cell spreading and migration over longer time scales (~1 hr). Harada et al. (2014) have previously suggested irreversible deformation of the nucleus in cells. In their experiments, nuclei in migrating cells must elongate to squeeze through tiny pores, and these elongated shapes persist in cells that express a high amount of A-type lamins to B-type lamins. However, it is possible that cells that migrate through pores remain elongated, causing the elongated nuclear shape to persist. This illustrates the difficulty in interpreting elongated nuclear

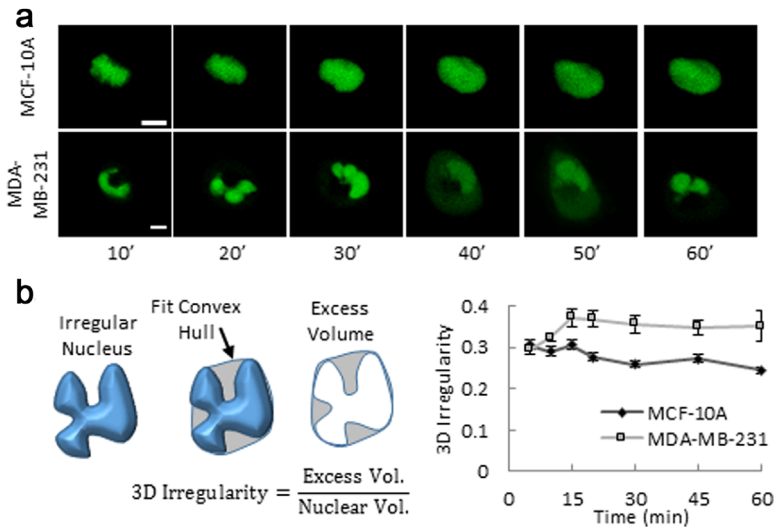

FIGURE 4 Cell spreading amplifies cancer nuclear abnormalities. (a) Shown is an example of nuclear shape changes during spreading of an MCF-10A and MDA-MB-231 cell. (b) Schematic shows the calculation of 3D irregularity defined here as the difference in volume between the nucleus and a convex hull fit to the nucleus divided by nuclear volume. Plot shows 3D irregularity plotted against time of spreading in MCF-10A and MDA-MB-231 cells. (n > 30 for both MDA-MB-231 and MCF-10A cells at each time point, error bars are standard error of the mean)

shapes as evidence for irreversible nuclear deformation without accounting for the cell shape.

Deguchi et al. (2005) quantified nuclear shapes after isolation from cells. However, their method involved chemical isolation and centrifugation; therefore, comparison of the *same* nucleus before and after isolation was not possible. Cao et al. (2016) modeled the nucleus as a hyperelastic shell containing permeable elastic chromatin. To explain the large plastic deformations of nuclei observed by Pajerowski et al. (2007) in cells lacking lamin A/C, they modeled chromatin as a plastic material surrounded by a much softer hyperelastic shell. But, as we point out here, the nucleus in wild-type fibroblasts—which contain normal levels of lamins (Alam et al., 2016)—is *irreversibly* deformed at steady state. The assumption of the elastic nucleus has not been previously tested by *removing* the forces on the nuclear surface (i.e., isolating the nucleus) and then tracking its shape. Yet several models have assumed that nuclear shapes reflect an elastic deformation (Allena, Thiam, Piel, & Aubry, 2015; Jean, Gray, Spector, & Chen, 2004; Kim et al., 2016; Li, Kumar, Makhija, & Shivashankar, 2014; Versaevel et al., 2012).

In our experiments, we excised the cell away from the nucleus, which exposed the nucleus to the cell culture medium. Although this may create an osmotic driving force for water flux into the nucleus (Finan, Chalut, Wax, & Guilak, 2009), such a change in osmotic pressure would cause an even faster relaxation of the nucleus to its original shape. Thus, an osmotic pressure—even if present—is not a confounding variable in our analysis.

We have modeled the mechanical behavior of the nucleus in cells by accounting for its bulk compressibility (volume elasticity) and the extensional modulus of the nuclear lamina (Li et al., 2015). While we cannot rule out a small change in nuclear volume in our excision experiments, we have previously shown that the volume of the nucleus stays approximately constant during nuclear flattening (Li et al., 2015). Similarly, Davidson, Sliz, Isermann, Denais, and Lammerding (2015) have reported that nuclear volume remains constant during nuclear deformations in cells lacking lamin A/C as they migrate through narrow pores. The lamina of a rounded nucleus has excess surface area stored in undulations and wrinkles (Li et al., 2015) and these decrease during the process of nuclear flattening (Neelam, Hayes, Zhang, Dickinson, & Lele, 2016). We therefore suggest that during nuclear flattening, the initially folded lamina becomes taut such that the surface area of the lamina remains constant. The lamina does not resist changes in nuclear shape until it becomes taut. Only when there is no more excess area in the lamina, does the lamina resist further nuclear elongation or flattening. Because a steady-state nuclear shape is reached upon cell spreading, it is likely that the taut lamina is too stiff to undergo extensions under typical cellular forces (Li et al., 2015). Consistent with this idea, Stephens, Banigan, Adam, Goldman, and Marko (2017) have found that the nucleus is initially soft to longitudinal strain due to mechanical resistance from chromatin, but is stiff beyond a threshold strain because of the nuclear lamina. We note that the elasticity of the nuclear lamina in cells (Dahl, Kahn, Wilson, & Discher, 2004) can become apparent when an external force stretches the (taut) nuclear lamina as is observed in short-time scale nuclear forcing experiments (Neelam et al., 2015; Pajerowski et al., 2007). But, it has not been demonstrated that forces generated by cells are sufficient to discernably extend the lamina.

Because nuclear deformation requires a *change* in cell shape, we speculate that this occurs due to a mechanical stress caused by frictional resistance in the cytoskeletal elements to expansion or contraction as the cell boundary moves relative to the nuclear surface (Li et al., 2015). What is the molecular mechanism of this transmission of stress? We have previously shown that cell spreading is necessary and sufficient to drive nuclear flattening in fibroblasts under a wide range of conditions (Li et al., 2015), including in the absence of microtubules, vimentin intermediate filaments, and myosin activity. Therefore, we speculate that it is primarily the F-actin network that transmits stress from the moving cell boundary to the nucleus. However, once F-actin is completely disrupted with pharmacological agents, any further changes in cell shape are not possible (Li et al., 2015), which makes it difficult to test the role of F-actin in mediating nuclear response to deformations in cell shape. Experiments which cause deformations in cell shape over time scales of minutes (typical time scales of migration and spreading) in the absence of F-actin will be needed to test whether the F-actin network is responsible for transmitting the dissipative stresses. Alternatively, it is possible that any of the three cytoskeletal filaments may transmit stresses to the nucleus, and disruption of one of these allows other structures to transmit the stresses. If there is such redundancy, then identifying the molecular structures that coordinate nuclear and cell shape is likely to remain a fundamental challenge.

Irrespective of the molecular source of the stress transmission, motion of the nuclear surface in response to motion of the cell boundary naturally allows the nucleus to mimic the cell shape. Thus, this mechanism can easily explain how the nucleus adopts an "hour-glass" shape when cells develop a similar shape during migration through narrow pores and constrictions (Friedl, Wolf, & Lammerding, 2011; Denais et al., 2016). Although it is possible that such extreme shapes result in stored elastic energy in the lamina, this is not required to explain the nuclear shape. We also note that once the nuclear shape is established during cell spreading or migration, actomyosin stress fibers can indent the apical surface of the nucleus as has been observed by others (Versaevel et al., 2014), and actin polymerization can constrict nuclei through narrow pores as observed in some cell types like dendritic cells (Thiam et al., 2016). Thus, multiple types of stresses can act in combination with stresses generated by motion of the cell boundary. However, it has not been shown that the resulting nuclear deformations by these types of stresses are reversible (i.e., elastic). Similarly, as shown here, the highly abnormal shapes of cancer nuclei are not necessarily an elastic response to cytoskeletal forces. Rather, the process of cell spreading can irreversibly amplify these abnormalities.

Why does dynamic cell spreading amplify nuclear abnormalities in cancer cells, but not in non-cancer cells (Figure 4d)? It has been suggested that the localization of lamins may be spatially inhomogeneous in cancer nuclei resulting in a mechanically "patchy" nuclear surface (Funkhouser et al., 2013). Thus, certain regions of the heterogeneous nuclear surface may be more compliant in response to mechanical stresses, resulting in

abnormal nuclear shapes. We note that knockdown of nuclear proteins other than the nuclear lamins (Lammerding et al., 2006) can also result in abnormalities—these include the chromatin remodeling protein Brg1 (Imbalzano, Imbalzano, & Nickerson, 2013) and endosome regulator protein Wash (Verboon et al., 2015).

Because gene expression and protein synthesis potentially depend on the physical properties of the nucleus (Cremer & Cremer, 2001; Swift et al., 2013; Thomas et al., 2002), irreversible deformations of the nucleus may trigger expression of genes during cell migration by modulating chromatin compaction (Tajik et al., 2016; Xiao, Freedman, Miller, Heald, & Marko, 2012). Cell-shape-dependent nuclear deformations may therefore enable (or at least contribute to) the known relationship between cell shape and cell function (Chen, Mrksich, Huang, Whitesides, & Ingber, 1997). Therefore, knowing how dynamic cell shape information is transmitted to the nucleus will be key to a complete understanding of the relationship between cell shape and cell function.

ACKNOWLEDGMENTS

This work was supported by funding from the National Institutes of Health (R01 GM102486 to TPL; R01 EB014869 to TPL and RBD; U54CA193419 to JDL; R01 CA172310 to HL) and the National Science Foundation (CMMI 1437395 to TPL).

COMPETING FINANCIAL INTERESTS

The authors declare no competing or financial interests.

REFERENCES

Alam, S. G., Zhang, Q., Prasad, N., Li, Y., Chamala, S., Kuchibhotla, R., ... Lele, T. P. (2016). The mammalian LINC complex regulates genome transcriptional responses to substrate rigidity. *Scientific Reports*, *6*, 38063.

Allena, R., Thiam, H., Piel, M., & Aubry, D. (2015). A mechanical model to investigate the role of the nucleus during confined cell migration. *Computer Methods in Biomechanics and Biomedical Engineering*, *18*(Suppl 1), 1868–1869.

Bloom, H. J., & Richardson, W. W. (1957). Histological grading and prognosis in breast cancer; a study of 1409 cases of which 359 have been followed for 15 years. *British Journal of Cancer*, *11*(3), 359–377.

Boyd, J., Pienta, K. J., Getzenberg, R. H., Coffey, D. S., & Barrett, J. C. (1991). Preneoplastic alterations in nuclear morphology that accompany loss of tumor suppressor phenotype. *Journal of the National Cancer Institute*, *83*(12), 862–866.

Bussolati, G., Marchiò, C., Gaetano, L., Lupo, R., & Sapino, A. (2008). Pleomorphism of the nuclear envelope in breast cancer: A new approach to an old problem. *Journal of Cellular and Molecular Medicine*, *12*(1), 209–218.

Cao, X., Moeendarbary, E., Isermann, P., Davidson, P. M., Wang, X., Chen, M. B., ... Shenoy, V. B. (2016). A chemomechanical model for nuclear morphology and stresses during cell transendothelial migration. *Biophysical Journal*, *111*(7), 1541–1552.

Chang, S. S., Guo, W. H., Kim, Y., & Wang, Y. L. (2013). Guidance of cell migration by substrate dimension. *Biophysical Journal*, *104*(2), 313–321.

Chen, C. S., Mrksich, M., Huang, S., Whitesides, G. M., & Ingber, D. E. (1997). Geometric control of cell life and death. *Science*, *276*(5317), 1425–1428.

Chow, K. H., Factor, R. E., & Ullman, K. S. (2012). The nuclear envelope environment and its cancer connections. *Nature Reviews Cancer*, *12*(3), 196–209.

Cremer, T., & Cremer, C. (2001). Chromosome territories, nuclear architecture and gene regulation in mammalian cells. *Nature Reviews Genetics*, *2*(4), 292–301.

Csucs, G., Michel, R., Lussi, J. W., Textor, M., & Danuser, G. (2003). Microcontact printing of novel co-polymers in combination with proteins for cell-biological applications. *Biomaterials*, *24*(10), 1713–1720.

Dahl, K. N., Kahn, S. M., Wilson, K. L., & Discher, D. E. (2004). The nuclear envelope lamina network has elasticity and a compressibility limit suggestive of a molecular shock absorber. *Journal of Cell Science 117*(Pt 20), 4779–4786.

Davidson, P. M., Sliz, J., Isermann, P., Denais, C., & Lammerding, J. (2015). Design of a microfluidic device to quantify dynamic intra-nuclear deformation during cell migration through confining environments. *Integrative Biology (Cambridge)*, *7*(12), 1534–1546.

Deguchi, S., Maeda, K., Ohashi, T., & Sato, M. (2005). Flow-induced hardening of endothelial nucleus as an intracellular stress-bearing organelle. *Journal of Biomechanics*, *38*(9), 1751–1759.

Denais, C. M., Gilbert, R. M., Isermann, P., McGregor, A. L., te Lindert, M., Weigelin, B., ... Lammerding, J. (2016). Nuclear envelope rupture and repair during cancer cell migration. *Science*, *352*(6283), 353–358.

Elston, C. W., & Ellis, I. O. (1991). Pathological prognostic factors in breast cancer. I. The value of histological grade in breast cancer: Experience from a large study with long-term follow-up. *Histopathology*, *19*(5), 403–410.

Finan, J. D., Chalut, K. J., Wax, A., & Guilak, F. (2009). Nonlinear osmotic properties of the cell nucleus. *Annals of Biomedical Engineering*, *37*(3), 477–491.

Friedl, P., Wolf, K., & Lammerding, J. (2011). Nuclear mechanics during cell migration. *Current Opinion in Cell Biology*, *23*(1), 55–64.

Funkhouser, C., Sknepnek, R., Shimi, T., Goldman, A., Goldman, R., & de la Cruz, M. (2013). Mechanical model of blebbing in nuclear lamin meshworks. *Proceedings of the National Academy of Sciences of the United States of America*, *110*(9), 3248–3253.

Giardina, C., Renzulli, G., Serio, G., Caniglia, D. M., Lettini, T., Ferri, C., ... Delfino, V. P. (1996). Nuclear morphometry in node-negative breast carcinoma. *Analytical and Quantitative Cytology and Histology*, *18*(5), 374–382.

Gundersen, G. G., & Worman, H. J. (2013). Nuclear positioning. *Cell*, *152*(6), 1376–1389.

Gupta, S., Marcel, N., Sarin, A., & Shivashankar, G. V. (2012). Role of actin dependent nuclear deformation in regulating early gene expression. *PLoS One*, *7*(12), 53031.

Harada, T., Swift, J., Irianto, J., Shin, J. W., Spinler, K. R., Athirasala, A., ... Discher, D. E. (2014). Nuclear lamin stiffness is a barrier to 3D migration, but softness can limit survival. *Journal of Cell Biology*, *204*(5), 669–682.

Haroske, G., Dimmer, V., Friedrich, K., Meyer, W., Thieme, B., Theissig, F., & Kunze, K. D. (1996). Nuclear image analysis of immunohistochemically stained cells in breast carcinomas. *Histochemistry and Cell Biology*, *105*(6), 479–485.

Imbalzano, A. N., Imbalzano, K. M., & Nickerson, J. A. (2013). BRG1, a SWI/SNF chromatin remodeling enzyme ATPase, is required for maintenance of nuclear shape and integrity. *Communicative & Integrative Biology*, *6*(5), e25153.

Jean, R. P., Gray, D. S., Spector, A. A., & Chen, C. S. (2004). Characterization of the nuclear deformation caused by changes in endothelial cell shape. *Journal of Biomechanical Engineering*, *126*(5), 552–558.

Khatau, S. B., Hale, C. M., Stewart-Hutchinson, P. J., Patel, M. S., Stewart, C. L., Searson, P. C., ... Wirtz, D. (2009). A perinuclear actin cap regulates nuclear shape. *Proceedings of the National Academy of Sciences of the United States of America*, *106*(45), 19017–19022.

Kim, D. H., Li, B., Si, F., Phillip, J. M., Wirtz, D., & Sun, S. X. (2016). Volume regulation and shape bifurcation in the cell nucleus. *Journal of Cell Science*, *129*(2), 457.

Lammerding, J., Fong, L. G., Ji, J. Y., Reue, K., Stewart, C. L., Young, S. G., & Lee, R. T. (2006). Lamins A and C but not lamin B1 regulate nuclear mechanics. *Journal of Biological Chemistry*, *281*(35), 25768–25780.

Li, Q., Kumar, A., Makhija, E., & Shivashankar, G. V. (2014). The regulation of dynamic mechanical coupling between actin cytoskeleton and nucleus by matrix geometry. *Biomaterials*, *35*(3), 961–969.

Li, Y., Lovett, D., Zhang, Q., Neelam, S., Kuchibhotla, R. A., Zhu, R., … Dickinson, R. B. (2015). Moving cell boundaries drive nuclear shaping during cell spreading. *Biophysical Journal*, *109*(4), 670–686.

McGregor, A. L., Hsia, C. R., & Lammerding, J. (2016). Squish and squeeze-the nucleus as a physical barrier during migration in confined environments. *Current Opinion in Cell Biology*, *40*, 32–40.

Neelam, S., Chancellor, T. J., Li, Y., Nickerson, J. A., Roux, K. J., Dickinson, R. B., & Lele, T. P. (2015). Direct force probe reveals the mechanics of nuclear homeostasis in the mammalian cell. *Proceedings of the National Academy of Sciences of the United States of America*, *112*(18), 5720–5725.

Neelam, S., Hayes, P. R., Zhang, Q., Dickinson, R. B., & Lele, T. P. (2016). Vertical uniformity of cells and nuclei in epithelial monolayers. *Scientific Reports*, *6*, 19689.

Pajerowski, J. D., Dahl, K. N., Zhong, F. L., Sammak, P. J., & Discher, D. E. (2007). Physical plasticity of the nucleus in stem cell differentiation. *Proceedings of the National Academy of Sciences of the United States of America*, *104*(40), 15619–15624.

Petrie, R. J., Koo, H., & Yamada, K. M. (2014). Generation of compartmentalized pressure by a nuclear piston governs cell motility in a 3D matrix. *Science*, *345*(6200), 1062–1065.

Schindelin, J., Arganda-Carreras, I., Frise, E., Kaynig, V., Longair, M., Pietzsch, T., … Cardona, A. (2012). Fiji: An open-source platform for biological-image analysis. *Nature Methods*, *9*(7), 676–682.

Stephens, A. D., Banigan, E. J., Adam, S. A., Goldman, R. D., & Marko, J. F. (2017). Chromatin and lamin A determine two different mechanical response regimes of the cell nucleus. *Molecular Biology of the Cell*, pp. mbc-E16.

Swift, J., Ivanovska, I. L., Buxboim, A., Harada, T., Dingal, P. C., Pinter, J., … Discher, D. E. (2013). Nuclear lamin-A scales with tissue stiffness and enhances matrix-directed differentiation. *Science*, *341*(6149), 1240104.

Tajik, A., Zhang, Y., Wei, F., Sun, J., Jia, Q., Zhou, W., … Wang, N. (2016). Transcription upregulation via force-induced direct stretching of chromatin. *Nature Materials*, *15*(12), 1287–1296.

Théry, M., & Piel, M. (2009). Adhesive micropatterns for cells: A microcontact printing protocol. *Cold Spring Harbor Protocols*, *2009*(7), 5255.

Thiam, H. R., Vargas, P., Carpi, N., Crespo, C. L., Raab, M., Terriac, E., … Piel, M. (2016). Perinuclear Arp2/3-driven actin polymerization enables nuclear deformation to facilitate cell migration through complex environments. *Nature Communications*, *7*, 10997.

Thomas, C. H., Collier, J. H., Sfeir, C. S., & Healy, K. E. (2002). Engineering gene expression and protein synthesis by modulation of nuclear shape. *Proceedings of the National Academy of Sciences of the United States of America*, *99*(4), 1972–1977.

Verboon, J. M., Rincon-Arano, H., Werwie, T. R., Delrow, J. J., Scalzo, D., Nandakumar, V., … Parkhurst, S. M. (2015). Wash interacts with lamin and affects global nuclear organization. *Current Biology*, *25*(6), 804–810.

Vergani, L., Grattarola, M., & Nicolini, C. (2004). Modifications of chromatin structure and gene expression following induced alterations of cellular shape. *The International Journal of Biochemistry & Cell Biology*, *36*(8), 1447–1461.

Versaevel, M., Braquenier, J. B., Riaz, M., Grevesse, T., Lantoine, J., & Gabriele, S. (2014). Super-resolution microscopy reveals LINC complex recruitment at nuclear indentation sites. *Scientific Reports*, *4*, 7362.

Versaevel, M., Grevesse, T., & Gabriele, S. (2012). Spatial coordination between cell and nuclear shape within micropatterned endothelial cells. *Nature Communications*, *3*, 671.

Webster, M., Witkin, K. L., & Cohen-Fix, O. (2009). Sizing up the nucleus: Nuclear shape, size and nuclear-envelope assembly. *Journal of Cell Science*, *122*(Pt 10), 1477–1486.

Xiao, B., Freedman, B. S., Miller, K. E., Heald, R., & Marko, J. F. (2012). Histone H1 compacts DNA under force and during chromatin assembly. *Molecular Biology of the Cell*, *23*(24), 4864–4871.

Zink, D., Fischer, A. H., & Nickerson, J. A. (2004). Nuclear structure in cancer cells. *Nature Reviews Cancer*, *4*(9), 677–687.

SUPPORTING INFORMATION

Additional Supporting Information may be found online in the supporting information tab for this article.

How to cite this article: Tocco VJ, Li Y, Christopher KG, et al. The nucleus is irreversibly shaped by motion of cell boundaries in cancer and non-cancer cells. *J Cell Physiol*. 2017;1–9. https://doi.org/10.1002/jcp.26031